Geomembrane displacement monitoring system installed in a multilayered cover at the Aldermac mine site

R. Faneva M. Rarison[1*], *James L.* Hanson[2], *Bruno* Bussière[1], *Mamert* Mbonimpa[1], *Nazli* Yesiller[2], and *Michel* Aubertin[3]

[1]Research Institute on Mines and the Environment (RIME), Université du Québec en Abitibi-Témiscamingue (UQAT), Rouyn-Noranda, Québec, Canada
[2]California Polytechnic State University, San Luis Obispo, California, United States of America
[3]Department of Civil, Geological and Mining Engineering, Polytechnique Montréal, Montréal, Québec, Canada

Abstract. The abandoned Aldermac mine site, located in the Abitibi-Témiscamingue region of Québec, Canada, is a former polymetallic mine that operated in the 1930s. Over the decades, the sulfidic mine wastes produced by the mine have been exposed to atmospheric conditions, leading to the generation of acid mine drainage (AMD) and contamination of the surrounding environment. In 2008–2009, reclamation works were initiated by the Québec government with the implementation of different techniques based on the characteristics of the different sectors of the mine site. In the southern sector, the production of AMD from the mine wastes pile is controlled by a multilayered cover system, including a 1.5 mm-thick textured high-density polyethylene geomembrane, aimed at limiting ingress of water and oxygen. In 2021, work was carried out to instrument the cover system with an innovative displacement measurement system that was developed and applied to the geomembrane along a sloping transect. The system allows continuous measurements of geomembrane displacement at three locations. This article discusses the installation of these instruments and presents preliminary results. Displacements over a 1-year monitoring period ranged from approximately 4 mm downslope to 32 mm upslope. This corresponded to strains ranged from approximately 0.01% contraction to 0.05% tension.

1 Introduction

In the mining industry, geomembranes (GMBs) are used during different phases of the mine life as a barrier to limit fluid migration. For example, GMBs can be used in operation as liners for heap leach pads (e.g., [1-3]) and tailings storage facilities (e.g., [4-6]). GMBs can also be integrated as a low hydraulic conductivity layer in cover systems at the reclamation stage (e.g., [7-9]). In cover systems, GMBs mainly act as a fluid (water and oxygen) barrier to limit contamination by acid mine drainage (AMD) and metal release from reactive mine wastes

* Corresponding author: faneva.rarison@uqat.ca

[7-10]. AMD is generated when sulfide minerals contained in mine wastes are exposed to atmospheric oxygen and water [11-13]. Sulfide oxidation reactions lead to a reduction in porewater pH, as well as the release of metals and sulfate [13]. Therefore, AMD discharge can lead to harmful impacts to the environment. By controlling ingress of water and oxygen with a cover system, AMD generation can be controlled, and the associated environmental impacts can be mitigated.

Tailings are fine-grained mine wastes generated during ore processing. These tailings are usually pumped at a relatively low solid content (<50% solids) into large storage areas called tailings storage facilities (TSFs). Tailings are susceptible to settling under their own weight due to their high water content [14]. This settlement of tailings can result in deformation of the cover system at the reclamation stage; this presents a significant concern when using a GMB [10], as it can introduce strain [15]. The strain in the GMB can lead to stress cracking, ultimately jeopardizing the integrity of the barrier, especially in the case of high-density polyethylene (HDPE) GMBs [15-17]. Therefore, a need exists to develop a monitoring system for tracking the displacement and corresponding strain of GMBs in mining cover systems placed on a TSF.

The measurement of localized strain in GMBs is complicated by several factors due to complications of fixing sensors to polymeric materials like GMBs. Traditional adhesives are often unsuitable, and alternative methods like thermal bonding can potentially alter GMB properties. Additionally, the presence of overlying materials complicates sensor access and measurement processes [18]. To the knowledge of the authors, no monitoring system is currently available to directly measure in situ strain in GMBs used in cover systems. To address this gap, a prototype system initially developed by Hanson, et al. [18] for liner applications has been adapted to suit the specific requirements of cover systems. To evaluate its effectiveness, this system was tested on an existing mine waste storage area where a cover system with a GMB was built to control AMD. This article aims at providing an overview of the work performed to develop the new monitoring system. First, the test site is presented, followed by a detailed description of the displacement measurement system and its installation. Preliminary results obtained during the first year of monitoring are then presented.

2 Methodology

2.1 Aldermac site description

The Aldermac mine site, located 15 km west of Rouyn-Noranda in the Abitibi-Temiscamingue region of Québec, Canada, was operated from 1932 to 1943 by Aldermac Mines Limited and the Aldermac Copper Corporation. The mine yielded various mineral resources including copper, gold, silver, silica, and pyrite. After the last operator's liquidation in January 1946, the site was abandoned, leading to the exposure of approximately 1.5 million metric tons of highly acid-generating tailings and waste rocks to atmospheric conditions [19]. Covering an area of approximately 76 ha, the abandoned mine site generated significant volumes of AMD and became one of the most problematic abandoned mine sites in the province of Québec. Efforts to mitigate the environmental impact began in 1982, with the construction of a dike in the southeast sector to contain pollutants and a bypass channel to divert uncontaminated water. However, the effects of the AMD persisted, leading to acidification and metal pollution of the surrounding water bodies. A second attempt to reduce the environmental impact of the site in 1995 involved construction of dikes around the tailings, and excavation and clean-up operations. Unfortunately, subsequent water analyses revealed minimal improvement in mitigation [19, 20].

In response to the persistent water contamination challenges, a third reclamation scenario was implemented between 2008 and 2009, dividing the Aldermac mine site into two main sectors for mine wastes storage. In the northern sector, the strategy employed featured a monolayer cover combined with an elevated water table. This approach was designed to limit oxygen availability and, consequently, reduce acid mine drainage (AMD) generation from the tailings [21-23].

Meanwhile, in the southern sector, a multilayered cover system, incorporating a GMB was constructed over acid-generating mine waste. The covered TSF has the shape of a mound, covering an approximate surface area of 5.2 ha, with a sloped section (with an average slope of approximately 4 to 5 horizontal to 1 vertical) surmounted by a flat section. The materials beneath the multilayered cover included tailings and excavated contaminated materials, which were placed using bulldozers without compaction, resulting in expected settlement. The main objective of the cover system was to restrict water and oxygen fluxes to limit the generation of AMD. [7-10].

More specifically, this multilayered cover system consists of four layers (see **Error! Reference source not found.**): a support layer of well-graded sand with gravel (0.30-m-thick), a low saturated hydraulic conductivity layer made of textured high-density polyethylene (HDPE) GMB (1.5 mm-thick) to prevent water movement, a protection layer of geotextile (3.5 mm-thick) to shield and support the GMB, and a surface layer of well-graded sand with gravel (1 m-thick and 1.4 m-thick on the flat section and on the slopes, respectively) as the top part of the cover system. In this type of cover system, the GMB performance predominantly determines the cover system effectiveness to control AMD generation.

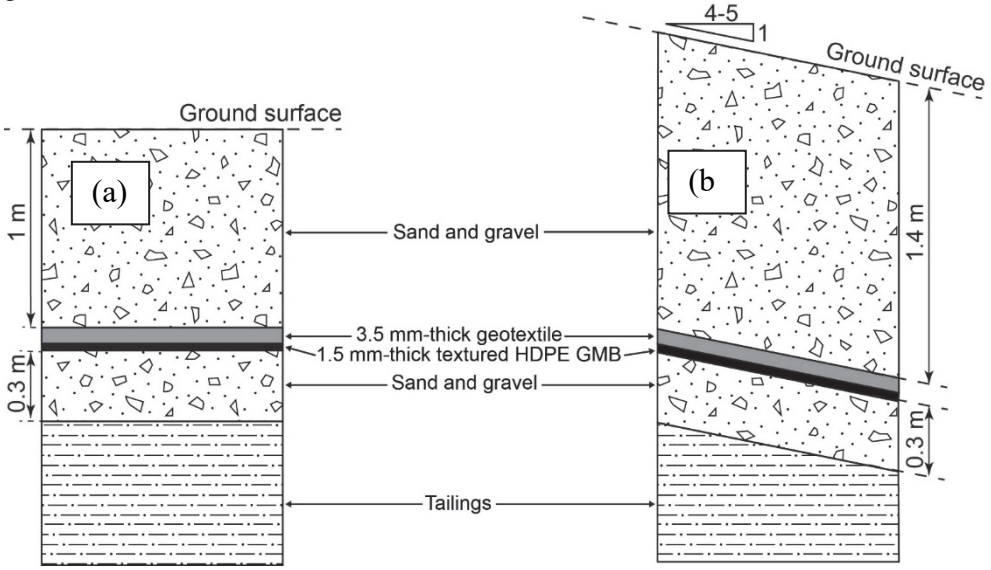

Fig. 1. Cross sections of the multilayered cover system built at the Aldermac mine site on the flat top section (a) and on the slopes (b).

2.2 TSF settlement evaluation

In 2012, as part of the monitoring program, four settlement plates were strategically positioned on the top surface of the TSF to track physical movement occurring within the area. Throughout the monitoring period, notable settlements were observed, indicating a certain degree of subsidence or movement within the containment cell. During the surveys of the settlement plates from 2012 to 2014, settlements of up to 13 cm were measured [24].

However, those settlement plates only provided local measurements of the settlement. In 2022, an aerial survey was included in the monitoring program to create a digital elevation model (DEM) of the containment cell and to follow its evolution every year. The DEM was generated from the cloud point obtained with an unmanned aerial vehicle (DJI Matrix 300) coupled with a DJI Zenmuse L1 light detection and ranging (LiDAR) system. The data processing was conducted with the geographic information system program ArcMap 10.1. Fig. 2a shows the map of the containment cell in September 2022, with the containment cell delimited by a black line, the outcrop contoured in yellow, the permanent path in grey, and the contour lines in red. The permanent path has been built outside the cover system, encircling it along its northern, eastern, and southern boundaries. It thus serves as a reference point since no settlement is expected at the level of the permanent path. The base map was generated with an orthophoto obtained during an aerial survey. The initial contour lines (in orange) from the as-built plan are presented in Fig. 2b. By comparing Fig. 2a and 2b, the modification of the shape of the containment cell can be seen clearly, especially a depression at the top of the cell caused by settlement of the tailings.

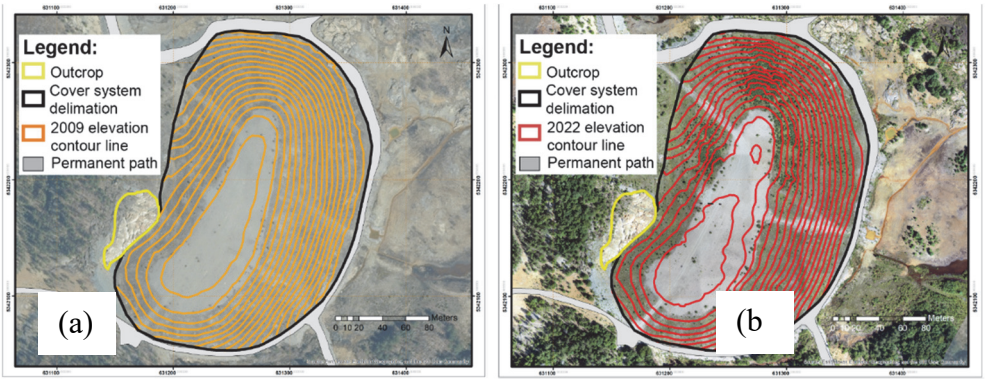

Fig. 2. Maps of the Aldermac mine waste storage area showing the comparison of the elevation contours from the as built plan (a) to the elevation contours in September 2022 (b).

This settlement affects the tensile stresses in the GMB, which could potentially affect its durability, for example by generating stress cracking of the GMB [15-17]. As the integrity of the GMB is crucial for effectively controlling AMD generation and ensuring the overall stability of the containment cell, understanding strain and stresses in the GMB is critical. Therefore, a GMB displacement system was developed, installed, and monitored.

2.3 Development of the geomembrane displacement measurement system

Measurement of the GMB displacement is based on a system developed by Hanson, et al. [18] for a GMB liner. The system is comprised of a linear potentiometer linked with a GMB coupon, which was welded onto the installed GMB. The wiring system consists of a stainless-steel braided wire that was encased within cross-linked polyethylene (PEX) tubing. This tubing serves a dual purpose: safeguarding the braided wire from potential damage caused by the protective layer and ensuring unhindered braided wire movement. A visual representation of this measurement system is depicted in Fig. 3.

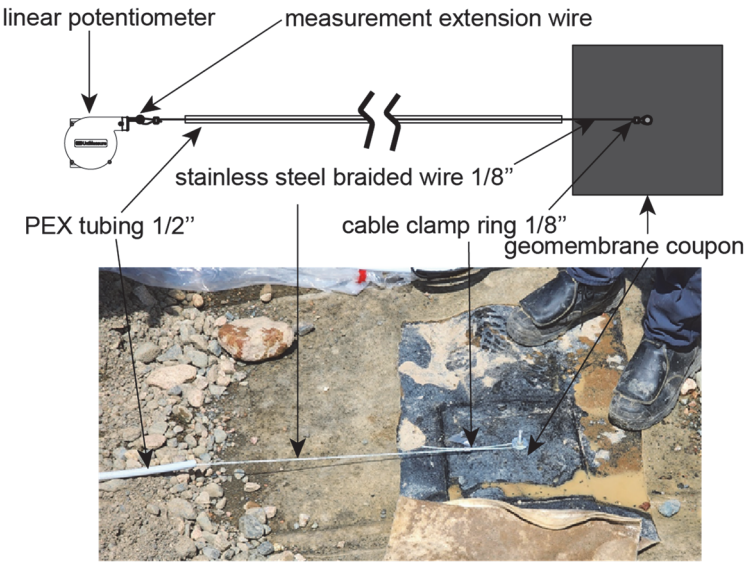

Fig. 3. Components of the geomembrane displacement measurement system.

The displacement (elongation/contraction) of the geomembrane is effectively transmitted as a translational movement to the linear potentiometer via the wiring system. This displacement is subsequently interpreted as a fluctuation in the electrical signal recorded at the level of the linear potentiometer. To obtain reliable measurements, the linear potentiometer is installed at a designated fixed point within a measurement box, which acts as a reference landmark. For this project, JX-P420-60-N11-20S-N1C linear potentiometers (from UNIMEASURE, USA) were used. These linear potentiometers provide a measurement range, determined by the length of the extension wire, of 60 in. (1,524 mm) with electrical responses (current intensity) ranging from 4 to 20 mA. The signal begins at 4 mA when the measuring tab is at its initial zero elongation position and culminates at 20 mA when fully extended to the 60-in. limit.

As it was not possible to fix a wire directly onto the installed GMB, a system of coupons was used, as presented in Fig. 3. The wire was fixed onto a metallic bolt with a washer on each side of the GMB coupon to maintain integrity. To limit interference, the coupon should have the same property as the installed GMB. A flat bolt was used to avoid any risk of indentation, and a cushion layer of GMB was installed between the bolt and the installed GMB. The GMB coupon is subsequently welded to the installed GMB by extrusion fillet following thermal welding. Fig. 4 shows the components of the coupon system with the different steps of the GMB coupon deployment onto the in-service GMB.

For data recording and monitoring, HOBO UX120-006M loggers from ONSET (USA) were integrated into the system and connected to the linear potentiometers (see Fig. 5). The logger has a precision rating of ± 0.001 mA. Consequently, the system has a theoretical displacement measurement precision of approximately ± 0.1 mm. This level of precision allows the system to potentially detect small displacements of the GMB, providing valuable insights into its performance.

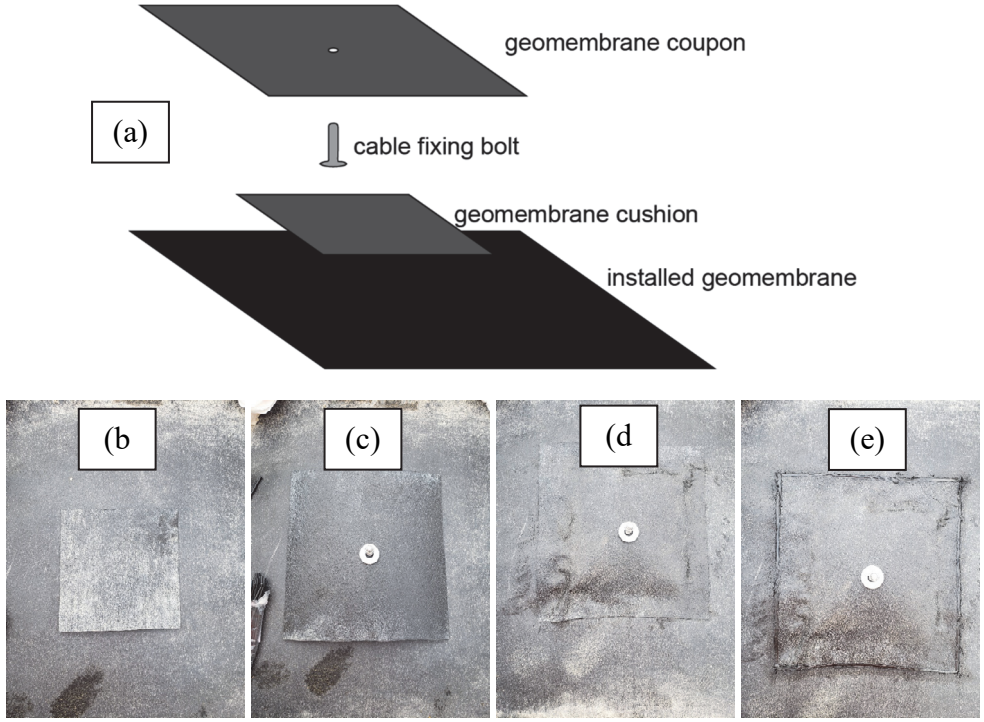

Fig. 4. Components of the geomembrane coupon (a) followed by the different steps of the installation: (b) GMB cushion installation, (c) GMB coupon installation, (d) thermal fusion, and (e) extrusion fillet.

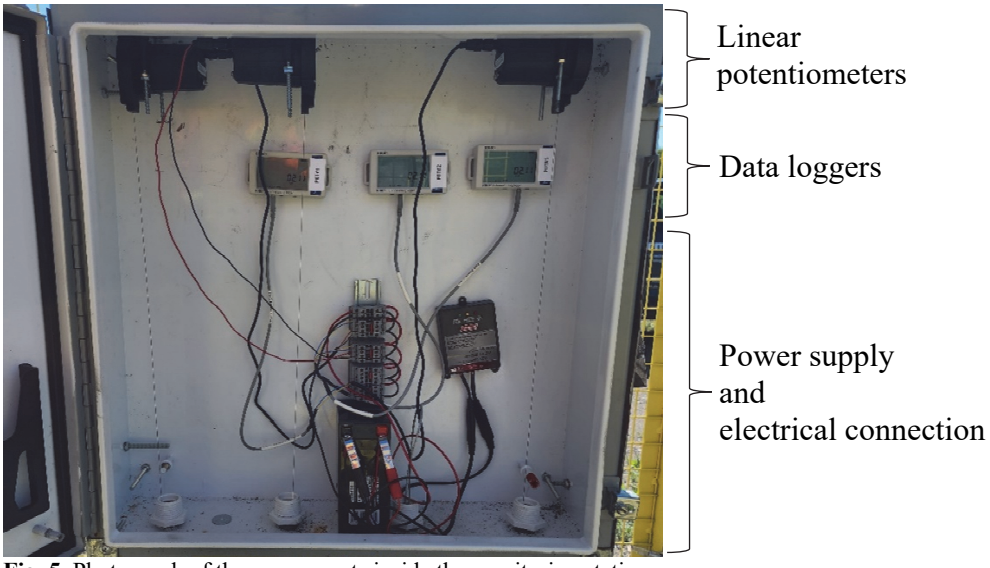

Fig. 5. Photograph of the components inside the monitoring station.

The measured displacement at time t (ΔL_{meas_t} in mm) calculated from the initial position is given by the following equation:

$$\Delta L_{meas_t} = (I_t - I_0) \times dl/A \quad (1)$$

where I_t is the current intensity (mA) registered at time t, I_0 is the initial current intensity (mA), and dl/A is the displacement per unit of current intensity (mm/mA). This last factor is specific to the linear potentiometer: for the linear potentiometer used in this study, this value was 95.25 mm/mA (obtained from preliminary testing).

The measured displacement includes any thermal expansion/contraction of the wire (ΔL_{wire_t}). To derive the geomembrane displacement (ΔL_{GMB_t}), it is necessary to apply a correction. The equations used to calculate the geomembrane displacement are as follows:

$$\Delta L_{GMB_t} = \Delta L_{meas_t} - \Delta L_{wire_t} \quad (2)$$

where:

$$\Delta L_{wire_t} = \alpha_{SS} \cdot L_{wire} \cdot \Delta T_t \quad (3)$$

where α_{SS} is the coefficient of thermal expansion of the stainless steel wire (17.3×10^{-6} mm/mm °C) [25], L_{wire} is the length of the wire (in mm), and ΔT_t is the wire temperature variation (in °C). The installation of temperature probe or thermocouple is needed at the geomembrane level to measure the wire temperature.

The global strain at a time t (ε_t) for a section between paired coupons can then be determined with the calculation of the quotient of the change in distance between two coupons at a time t ($\Delta L_{coupons_t}$) and the initial linear distance between two coupons ($L_{coupons_0}$), following the equation:

$$\varepsilon_t = \frac{\Delta L_{coupons_t}}{L_{coupons_0}} \quad (4)$$

2.4 Installation of the geomembrane displacement measurement system

To evaluate the response of the entire slope length of the cover system, three coupons (top, middle, and bottom) were placed along a transect on the east side of the Aldermac mine waste storage area. The linear spacing along the slope between the coupons was 50 m for top/middle and 25 m for middle/bottom, and 25 m for bottom/monitoring station. This transect followed an approximate west to east direction, had a relatively gentle slope and the installation had minimal impact on vegetation. As some settlement has been observed at the crest of the cell, the decision was made to install the monitoring station at the bottom of the slope, near the permanent path. Fig. 6 shows a map with the location of the three coupons and the monitoring station.

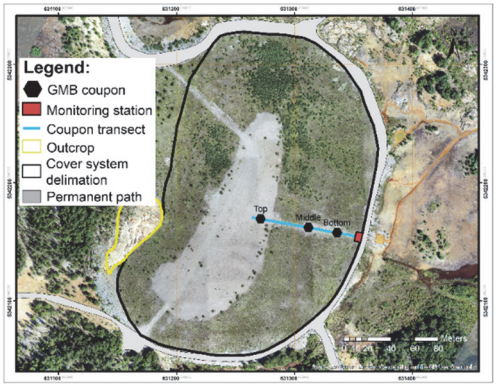

Fig. 6. Map with the locations of the geomembrane coupons and the monitoring station.

The field monitoring program was developed in two steps: the first step conducted in October 2021 was to install the bottom and middle coupons, while the second step in June 2022 was to complete the installation of the top coupon. As the cell was already in service, a trench was excavated along the sloping transect from the location of the monitoring station. The coupon system was then installed and welded to the GMB (see Fig. 4). The wiring system was deployed along the geotextile level, just above the GMB (cf. **Error! Reference source not found.**), and the tension of the braided wire was adjusted to correspond to a signal of approximately 12 mA from the linear potentiometer. Initiating the linear potentiometer halfway through its range allows displacement to be detected both downslope and upslope movements of GMB. Once the system was set, the protection layer was replaced, and data logging began.

3 Preliminary results

For the monitoring period from 2022-07-01 to 2023-07-01, the measured displacements are presented in Fig. 7. The measured displacements of the top, middle, and bottom coupons varied from –4 to +6, –2 to 3, and –8 to 1 mm, respectively.

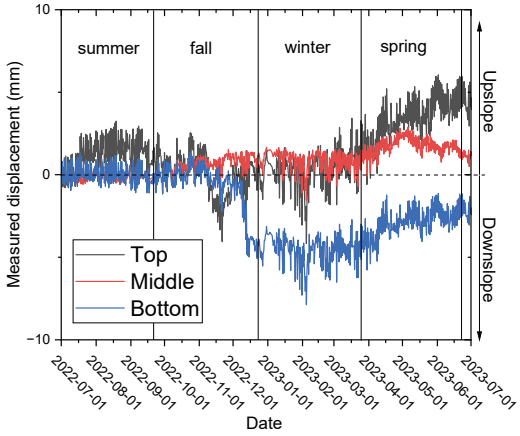

Fig. 7. Measured displacement from July 2022 to July 2023.

Fig. 8a illustrates the correction required obtain the GMB coupon displacements from the measured displacements, while the Fig. 8b depicts the temperature at the GMB level. The correction is directly proportional to temperature, and its magnitude increases with the length of the wire, as indicated by Equation 3. This correction ranges from approximately 5 mm of expansion to approximately 25 mm of contraction.

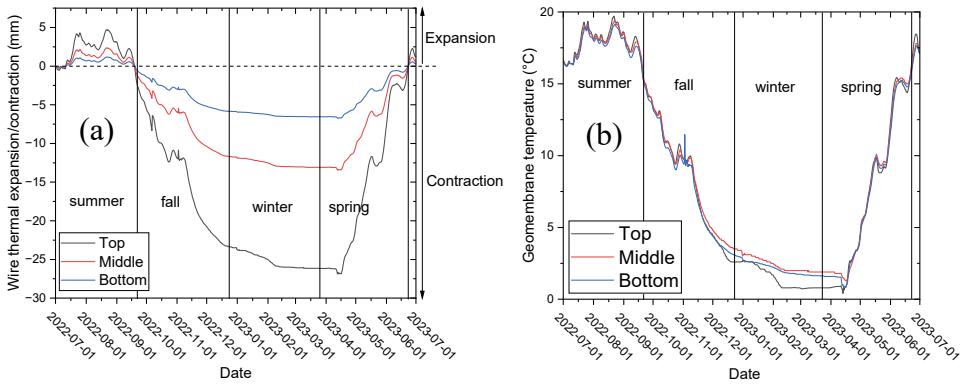

Fig. 8. Wire thermal expansion/contraction (a) and the temperature at the geomembrane level (b) from July 2022 to July 2023.

Fig. 9 presents the geomembrane coupon displacement achieved by applying the correction (as shown in Fig. 8) to the raw measured displacement data (depicted in Fig. 7). In Fig. 9, negative values correspond to downslope movements, while positive values correspond to upslope movements. The correction is significant in comparison to the measured displacements. The top coupon exhibits displacements ranging from approximately 4 mm downslope to 32 mm upslope. The middle coupon demonstrates movements spanning from approximately 3 mm downslope to 16 mm upslope. Lastly, the bottom coupon displays displacements ranging from approximately 3 mm downslope to 5 mm upslope. The GMB generally exhibited an upslope movement starting in the early fall, coinciding with cooler temperatures. Conversely, the GMB demonstrated downslope movement beginning in early spring, corresponding to the onset of warmer temperatures.

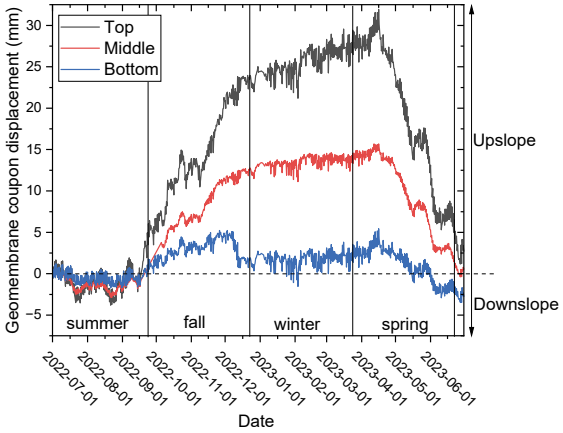

Fig. 9. Geomembrane coupon displacement.

Fig. 10 displays the overall strains calculated between paired coupons, including Top-Middle, Middle-Bottom pairs, and Bottom coupon-Monitoring station Within this figure, positive values signify GMB tension, whereas negative values denote GMB contraction. The results reveal that the calculated values are low, ranging from approximately 0.008% contraction to 0.05% tension. The findings suggest that GMB strains are temperature dependent and display a seasonal pattern. Over the course of a year, there is a tendency for these strains to revert to their initial state.

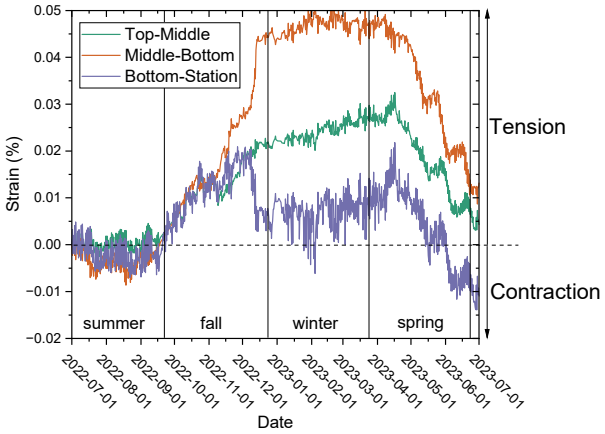

Fig. 10. Calculated strains between paired coupons, and the bottom coupon/measurement box.

4 Summary and conclusions

This paper documents a new setup for the measurement of the geomembrane displacement developed for geomembrane in multilayered covered system. This setup was tested along a transect equipped with three geomembrane coupons (top, middle, and bottom) spaced at intervals of 50 m and 25 m, respectively.

The following conclusions are drawn from this investigation:

- The new setup has proven its capability to measure GMB displacements (on the order of mm), highlighting its precision.
- The measured displacements ranged from approximately 4 mm downslope to 32 mm upslope over the 1-year monitoring period.
- The significance of thermal correction of the measurement wire was evident (ranging from 27 mm contraction to 5 mm expansion). Applying the thermal correction is particularly important when working with long wire lengths exposed to important temperature variations.
- The calculated strains ranged from approximately 0.008% contraction to 0.05% tension over the 1-year monitoring period.
- The overall response of the GMB slope was highly temperature-dependent with seasonal patterns of displacements and strains observed, underscoring the value of deploying a system such as that described in this paper for detailed continuous monitoring of GMB performance in service.

The research program presented in this paper was supported by the "*Fond de Recherche du Québec – Nature et Technologies (FRQNT)*" of the Québec Government, Canada, Laronde Mining Complex by Agnico Eagle, Éléonore Mine by Newmont, and Raglan Mine by Glencore. The authors also acknowledge the "*Ministère des Ressources Naturelles et des Forêts (MRNF) du Québec*", Canada, who granted the access to the site.

References

1. J. F. Lupo, Geotext. Geomembr., **28**, 163 (2010)
2. R. Thiel and M. E. Smith, *Geotext. Geomembr.,* **22**, 555 (2004)
3. N. Touze-Foltz and J. Lupo, Rev. Sci. Eaux & Territ., **Spécial Ingénieries EAT-28**, 101 (2009)
4. S. Gulec, C. Benson, and T. Edil, J. Geotech. Geoenvironmental Eng., **131**, 937 (2005)

5. R. K. Rowe, P. Joshi, R. W. I. Brachman, and H. McLeod, J. Geotech. Geoenvironmental Eng., **143**, (2017)
6. A. Tuomela, A.-K. Ronkanen, P. M. Rossi, A. Rauhala, H. Haapasalo, and K. Kujala, Geosci., **11**, 93 (2021)
7. A. Maqsoud, B. Bussière, and M. Mbonimpa, *Low Saturated Hydraulic Conductivity Covers*, in *Hard Rock Mine Reclamation*, B. Bussière and M. Guittonny Eds., 93 (2021)
8. N. Yesiller, J. L. Hanson, B. Bussière, T. Pabst, and M. Aubertin, *Use of Geomembranes in Reclamation Covers for Reactive Mining Waste Disposal Sites*, in Proceedings of GeoEdmonton 2018, Edmonton, Alberta, Canada (2018)
9. R. F. M. Rarison, M. Mbonimpa, B. Bussière, and S. Pouliot, Int. J. Geosynth. Ground Eng., **9**, 1 (2022)
10. M. Aubertin, B. Bussière, T. Pabst, M. James, and M. Mbonimpa, *Review of the Reclamation Techniques for Acid-Generating Mine Wastes upon Closure of Disposal Sites*, in Proceedings of GeoChicago 2016. Chicago, Illinois, USA, 343 (2016).
11. D. W. Blowes et al., *The Geochemistry of Acid Mine Drainage*. (2014)
12. D. K. Nordstrom, D. W. Blowes, and C. J. Ptacek, Appl. Geochem., **57** (2015)
13. B. Plante, G. Schudel, and M. Benzaazoua, *Prediction of Acid Mine Drainage*, in *Hard Rock Mine Reclamation*, B. Bussière and M. Guittonny Eds., 21 (2021)
14. B. Bussiere, Can. Geotech. J., **44**, 1019 (2007)
15. R. K. Rowe and Y. Yu, Geotext. Geomembr., **47**, 439 (2019)
16. J. Scheirs, *A guide to polymeric geomembranes: a practical approach*. John Wiley & Sons (2009)
17. W. W. Müller and A. Wöhlecke, Environ. Geotech., **6**, 162 (2019)
18. J. L. Hanson, M. T. Onnen, and N. Yesiller, *In-Situ Deformation Measurements for Geomembranes in Landfill Liners*," in Proceedings of the Geosynthetics 2013, April 1-4, 2013, Long Beach, California, USA (2013)
19. J. Cyr, R. Maurice, and D. Isabelle, *Restauration du site minier Aldermac*, in Proceedings of the Symposium Rouyn-Noranda: Mines and the Environment, Rouyn-Noranda, Québec, QC, Canada, (2011)
20. I. Bédard, *Techniques de rehabilitation des zones d'epanchement du parc a residus miniers Aldermac* [Mémoire de maîtrise, Département des génies civil, géologique et des mines, École Polytechnique de Montréal, Université de Montréal, PolyPublie. https://publications.polymtl.ca/8739/] (2002)
21. T. Pabst, *Elevated Water Table with Monolayer Covers*, in *Hard Rock Mine Reclamation*. Bussière and M. Guittonny Eds., 187 (2021)
22. A. Maqsoud, M. Mbonimpa, M. Benzaazoua, and S. Turcotte, Mining, **2**, 65 (2022)
23. M. Ouangrawa, M. Aubertin, J. W. Molson, B. Bussière, and G. J. Zagury, Wat. Air. & Soil Poll., **213**, 437 (2010)
24. A. Maqsoud, M. Mbonimpa, and B. Bussière, *Restauration du site minier Aldermac : instrumentation et suivi de l'efficacité - Rapport final,* Unité de Recherche et de Service en Technologie Minérale URSTM (2015)
25. E. Oberg, F. D. Jones, H. L. Horton, and H. H. Ryffel, *Machinery's Handbook 27th Edition: A Reference Book for the Mechanical Engineer, Designer, Manufacturing Engineer, Draftsman, Tookmaker, and Machinist*. New York, USA, Industrial Press Inc., (2004)